Original Study **Open Access**

Muhammad Tariq Bashir*, Muhammad Imad, Hamza Jamal*, Md. Munir Hayet Khan, Md. Alhaz Uddin, Bakht Zamin, Faizan Farid, Hamza Ahmad Qureshi

Assessing the Impact of Varying Fines and Antistripping Agent on Moisture Susceptibility in Asphalt Concrete Mixtures

https://doi.org/10.2478/sgem-2024-0018
received February 5, 2024; accepted July 4, 2024.

Abstract: Sustainable infrastructural development is vital for both developed and developing countries. The primary concern in hot mix asphalt (HMA) pavements is related to damages caused by moisture. This research makes efforts to evaluate the moisture susceptibility of a dense-graded surface HMA mixture using simple performance tests (SPTs) and Superpave indirect tensile tests (IDTs). Coating of fines (dust) on the aggregate can prevent the asphalt binder from bonding directly to the surface of the aggregate. Therefore, SPT and IDT have been performed by varying the proportion of fines (3%, 6%, and 9%) in the mix. For each proportion of fines, the optimum asphalt content was determined and used for further preparation of test specimens. The addition of hydrated lime [$Ca(OH)_2$] to asphalt mixtures improved the adhesive bond between aggregate and bitumen, as well as reduced the occurrence of stripping. In addition, when aggregates coated with clays, hydrated lime with a pozzolanic ally to remove those deleterious materials. The amount of antistripping agent incorporated was 1.5% by weight of dry aggregate, a proportion commonly used in the industry for such applications. Standard Marshall Mix design procedure was employed to design the asphalt mixtures. The laboratory investigation and subsequent statistical analysis were conducted using Minitab-15 software, which yielded significant insights into the effectiveness of hydrated lime as an antistripping additive in asphalt concrete mixtures. The findings indicate that incorporating hydrated lime substantially facilitates mitigating moisture-induced stripping in asphalt mixtures.

Keywords: Hot Mix Asphalt; Superpave Gyratory Compactor; Simple Performance Test; Indirect Tensile Test.

1 Introduction

In recent years, the transportation sector has encountered tremendous challenges in improving the durability and performance of asphalt concrete mixtures (Guo et al., 2022; Karimi et al., 2023). A primary composition of hot mix asphalt is bitumen and aggregate, and the performance of asphalt concrete pavement (ACP) is largely dependent on the dynamic interaction between these essential components. Including fine particles significantly impacts the constitution and functionality of concrete and asphalt amalgams (e.g., asphalt content, elasticity, fracture). The robustness and load-bearing capability of hot mix asphalt (HMA) stem from forming an aggregate framework facilitated by particle–particle interaction and interlocking (Kalaitzaki et al., 2017). The combined chemical and physical properties of bitumen and aggregate control the overall behaviour of the asphalt concrete mixture (Asmara, 2023; Tang et al., 2023). Notably, during the mixing process, heated bitumen covers and penetrates the pores of the aggregate particles. However, granite–asphalt pavement constructed using

***Corresponding authors: Muhammad Tariq Bashir,** Department of Civil Engineering, CECOS University of IT and Emerging Sciences, Peshawar, Pakistan; Faculty of Engineering and Quantity Surveying (FEQS) INTI International University, Persiaran Perdana BBN, Nilai 71800, Negeri Sembilan, Malaysia, E-mail: tariqbashir@cecos.edu.pk; **Hamza Jamal,** Department of Civil Engineering, CECOS University of IT and Emerging Sciences, Peshawar, Pakistan, E-mail: hamzajamal@cecos.edu.pk
Muhammad Imad, Faizan Farid, Hamza Ahmad Qureshi, Bakht Zamin, Department of Civil Engineering, CECOS University of IT and Emerging Sciences, Peshawar, Pakistan
Md. Munir Hayet Khan, Faculty of Engineering and Quantity Surveying (FEQS) INTI International University, Persiaran Perdana BBN, Nilai 71800, Negeri Sembilan, Malaysia
Md. Alhaz Uddin, Department of Civil Engineering, College of Engineering, Jouf University, Sakakah 72388, Saudi Arabia

conventional methods exhibits issues such as asphalt film stripping from the aggregate, particle fallout, and general looseness that leads to other water damage (Ghani et al., 2022; Ye et al., 2022).

Moreover, the prolonged exposure of asphaltic pavements to moisture and atmospheric precipitation initiates a process where water interaction causes bond failure within the asphalt matrix. This degradation process, known as stripping, leads to the disintegration of the asphaltic mixture and compromises its structural integrity (Abed et al., 2019; Cong et al., 2021). Numerous studies have reported that moisture damage in asphalt concrete manifests in two primary ways: through moisture infiltration at the asphalt–aggregate interface, causing adhesive failure, and by the permeation of moisture into bitumen (Guo et al., 2022; Pezowicz & Choma-Moryl, 2015). This reduces the cohesive strength and leads to cohesive failure. This phenomenon, often called moisture damage, reduces the asphalt mixture's stiffness, strength, and durability (Abed et al., 2019; Bashir et al., 2020; Park et al., 2017).

The use of additives is a technique adopted to enhance pavement properties. Among these, hydrated lime has emerged as a promising additive due to its wide availability and relative affordability compared to other modifiers like polymers (Al-Tameemi et al., 2015). It is considered a significant additive in asphalt mixtures as it enhances the adhesive bonding between asphalt and aggregates by reducing the potential for moisture damage. The adhesion of the bituminous film over the aggregate surface is crucial for increasing durability of the bituminous pavement (Alam & Aggarwal, 2020). Depletion of the bituminous film from the hydrophilic aggregate surface due to the presence of water is known as stripping. The addition of lime not only mitigates the moisture sensitivity of HMA and increases its stiffness without significantly increasing the brittleness of bitumen (Faramarzi et al., 2017; Sukhija et al., 2023), but has also been proven more effective than inert fillers in stiffening asphalt concrete mixtures at high temperatures. The method of incorporating hydrated lime into asphalt mixtures is crucial as it may coat the aggregate surface by altering its bonding positions from acidic to basic (Diab & Enieb, 2018; Kaseer et al., 2019). This change strengthens the aggregate and bitumen attachment and prevents moisture-induced separation. In addition, the interaction of hydrated lime with the acidic components of bitumen forms insoluble calcium salts, which further protect the adhesive bond by preventing harmful soap formation in the binder (Kaseer et al., 2019).

In short, the role of material science in developing sustainable infrastructures is crucial. Hydrated lime, a significant component in asphalt mixes, influences the moisture vulnerability of HMA pavements. Subsequently, it reduces the strength and durability of asphalt pavements due to water infiltration between the asphalt mixture particles (Abed et al., 2019). This study explores the engineering properties of asphalt cement and the impact of moisture-induced damages on the failure of asphalt paving mixtures that leads to significant financial loss in highway construction. Moreover, the research studies the primary function of anti-stripping additives in enhancing the bond between aggregate and bituminous binder in HMA, emphasizing the effectiveness of hydrated lime as an anti-stripping agent. In addition, it explores the combined effect of the quantity of fines and lime modification on the strength and stiffness of asphaltic mixtures, which contribute to a deeper understanding of mitigating moisture-induced damages and control in asphalt mixtures.

2 Materials and Methods

Marshall Mix design (MMD), a highly precise methodology for determining optimum asphalt contents, was meticulously prepared and repeated thrice by varying the proportions of fines (3%, 6%, and 9%) employing National Highways Authority (NHA) gradation B. The number of fines (passing No. 200 sieve) in NHA gradation B is 5.5%. When the amount of fraction passing the No. 200 sieve is 3%, the sum of material from sieve 3/4″ to sieve No. 200 is 97%. In the second set of conditions, the passing No. 200 sieve is 6%, so the material from sieve 3/4″ to No. 200 sieve is 94%, similar to the 9% fines mixture. The amount of hydrated lime used as a mixture modifier was kept at 1.5% of the dry weight of aggregates. Hydrated lime was introduced in its dry form to hot aggregates and thoroughly mixed before applying a binder to prepare specimens. The parameters analysed included strength, stiffness, and moisture sensitivity. In addition, the prepared HMA specimens underwent a freeze–thaw cycle following ASTM D4867 to evaluate their susceptibility to moisture.

2.1 Selection of Materials

The materials for testing included Margalla aggregates, and the aggregate gradation adhered to NHA class B specifications for dense-graded surface course mixtures. In Pakistan, numerous governmental and nongovernmental road construction agencies commonly utilize a penetration grade of 60/70 bitumen for flexible

Table 1: Sieve size with different percentages of fines.

Sieve size	Gradation with 3% fines		Gradation with 6% fines		Gradation with 9% fines	
	% Passing	% Retained	% Passing	% Retained	% Passing	% Retained
3/4”	100	0	100	0	100	0
1/2”	80	20	85	15	86	14
3/8”	67	13	70	13	74	12
#4	47	20	57	20	54	20
#8	28	19	37	20	34	20
#16	9	19	17	20	14	20
#200	4	5	12	5	9	5
Pan		3		6		9

pavement construction. Consequently, penetration grade 60/70 bitumen was employed for this research, and the specific batch used in the study was sourced from Attock Refinery Limited (ARL) in Rawalpindi, Pakistan.

The maximum aggregate size for surface course mixtures was 3/4 inch (19.0 mm). The aggregates of different sizes (coarse and fine) brought from the Margalla crush plant were sieved based on ASTM standard C 136. The quantity of fines passing through the No. 200 sieve was transformed by 3%, 6%, and 9% within NHA gradation B. As a result, three distinct gradations were formulated, each exhibiting slight differences in the percentages of fines, as illustrated in Table 1.

2.2 Preparation of Bituminous Mixes

Bituminous mixes were prepared according to ASTM D 6926 (Standard, 2015), which is standard practice for preparing bituminous specimens using the Marshall apparatus. The optimum asphalt contents for each type of gradation were determined thrice by revising the MMD procedure. The volumetric properties, stability, and flow were measured and verified using the MMD criterion.

For each combination of asphalt cement and aggregates, a total of three specimens were prepared. Considering the three types of gradations with varying percentages of fines (3%, 6%, and 9%), 15 specimens were prepared for each type. Therefore, the overall number of specimens amounted to 45. To assess the impact of different binder contents on the mixture, specimens were prepared at five distinct binder contents such as 3.5%, 4.0%, 4.5%, 5.0%, and 5.5%. After removing the dried aggregates and heated bitumen from the oven, they were immediately transferred into the mechanical mixing machine. The range of mixing temperature was kept at 160°C and 165°C, corresponding to the temperature during the manufacturing of bituminous mixes in Pakistan (NHA specifications). Moreover, this mixing temperature corresponds to the binder viscosity range of 0.17 ± 0.02 Pa, as specified by the Superpave mix design (SP-2). Each bituminous mix prepared using a mechanical mixing machine was transferred and placed in a metal container (Figure 1).

The volumetric properties of the mix, including voids in mineral aggregates (VMA), voids filled with asphalt (VFA), air voids (Va), and unit weight, were calculated by their respective formulas after the determination of theoretical maximum specific gravity (Gmm) and bulk specific gravity (Gmb). Theoretical maximum specific gravity (Gmm) and bulk specific gravity (Gmb) of bituminous paving mixtures were determined following ASTM D2041 (ASTM, 2011) and ASTM D2726 (ASTM International, 2021). After Gmb was determined, the specimens were placed in the water bath for 1 hour at 60°C and then tested for stability and flow. The specimen was loaded at a constant deformation rate of 5 mm/min until failure. The total maximum load in N (that causes specimen failure) is taken as Marshall stability. The total amount of deformation in units of 0.25 mm that occurs at the maximum load was recorded as the flow number value. The specimen was tested immediately after removing it from the water bath.

The job-mix formula (JMF) obtained from MMD were utilized for preparing specimens for resilient and dynamic modulus. After sieve analysis, the aggregates were dried to a constant weight at 105°C–110°C. The specimens for dynamic modulus were prepared according to ASTM D 3496 using a gyratory compactor (ASTM, 2020). The compaction was controlled by a total of 125 number of gyrations. Hydrated lime with 1.5% of the dry weight of aggregates was mixed into 12 specimens before the application of bitumen. For the dynamic modulus test,

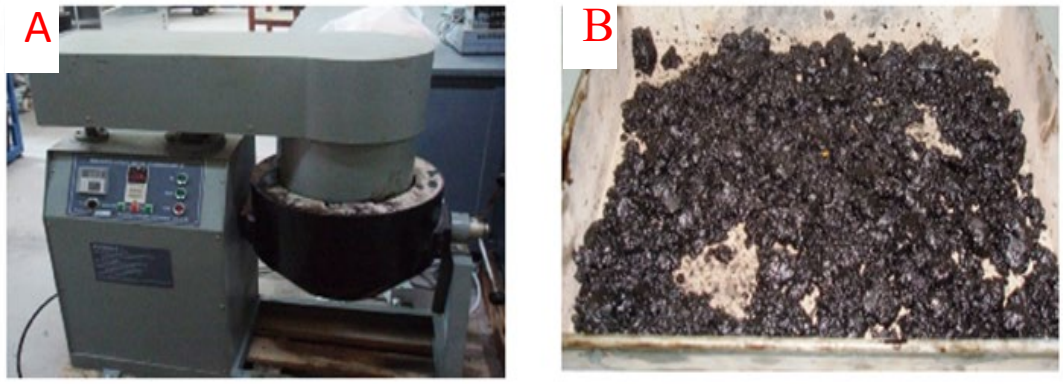

Figure 1: A) Mixing of aggregates and bitumen in a mechanical mixing machine, B) loose mixture prepared for conditioning.

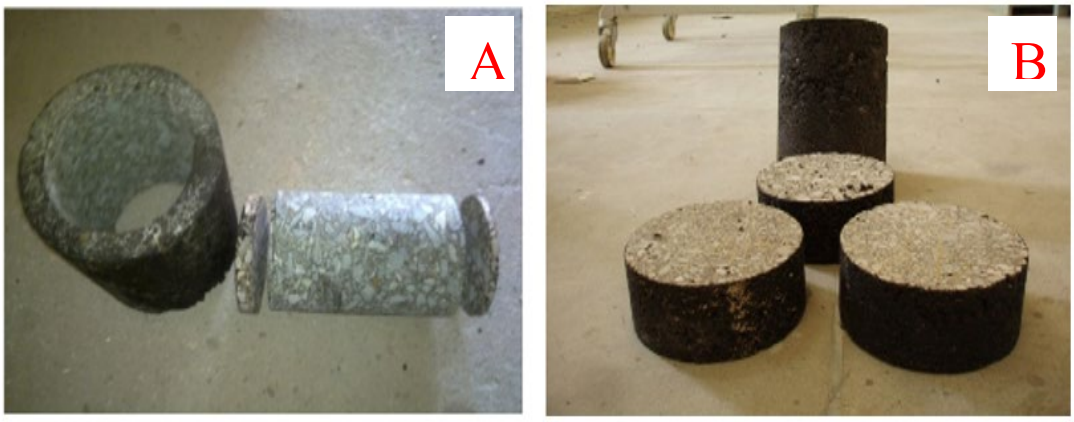

Figure 2: A) Core and trimmed specimen along with waste rings for SPT; B) core specimens for IDT.

cylindrical samples with 188 mm height and 150 mm diameter were compacted by the Superpave gyratory compactor (SGC). The core cutter machine observed the centre of the gyratory specimen's 4″ diameter, and the specimen was trimmed on both ends to 6″ height (Figure 2).

2.3 Determination of indirect tensile strength

The indirect tensile strength value is used to determine the resilient modulus of bituminous paving mixes (Table 2). The procedure adopted for determining indirect tensile strength followed ASTM D4867, which is essential to evaluate the moisture susceptibility potential of asphalt concrete mixtures. The tensile strength of both subsets (control and lime-modified mixtures) was determined at 25°C. The specimen was placed into the loading apparatus, and the loading strips were positioned to be centred in the vertical plane and parallel to each other. The stress–strain test was conducted by applying a diametric load at 50 mm/min. The stress at which failure occurred was recorded as the indirect tensile strength of the specimen. 20% of that peak load value of the indirect tension test was taken for the resilient modulus test.

After determining indirect tensile strength, the actual resilient modulus tests were performed. The specimen was loosely fitted into the jig on the bottom loading platen. The height of the cross arm was adjusted, so that the linear variable displacement transducer (LVDT) remained precisely in line with the horizontal centre of the specimen. The specimen was transferred into the universal testing machine for the resilient modulus test. All specimens were conditioned and tested at 25°C. The peak loading force was kept at 20% of the failure load, and the seating force was taken as 10% of the peak loading force as specified by ASTM D4123 (Brown & Foo, 1989). The value of Poisson's ratio was assumed to be 0.4. When the target test temperature was reached, the load pulse

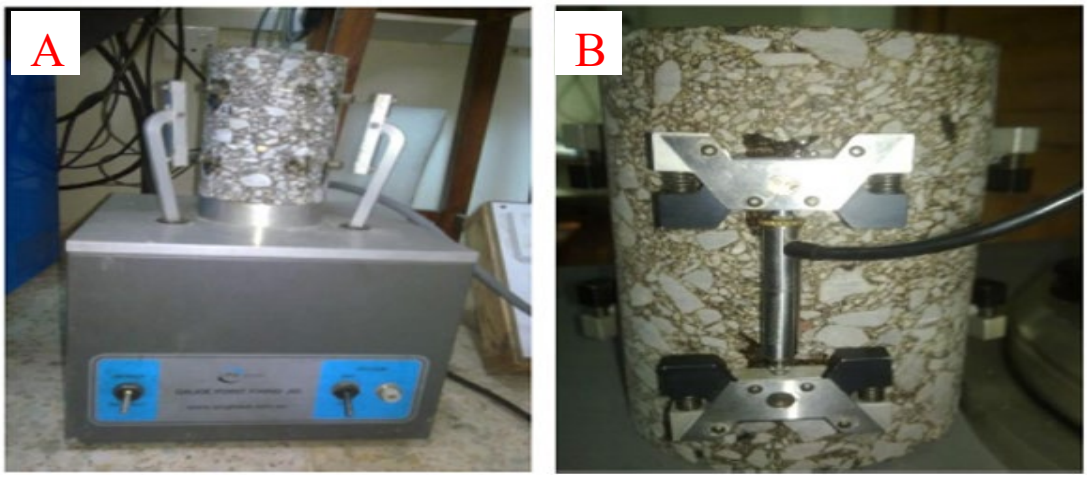

Figure 3: A) Studs fixing using gauge point fixing device; **B)** clamps and LVDTs mounted on the sample.

Table 2: Peak load values in indirect tensile strength test.

Fines	Controlled unconditioned	Controlled conditioned	Antistripped and conditioned
3%	9200 (N)	7200 (N)	8000 (N)
6%	9500 (N)	7600 (N)	8500 (N)
9%	9100 (N)	7000 (N)	7700 (N)

repetition period, pulse width, and conditioning pulse count were input, the test started, and the specimen was subjected to haversine loading. As the conditioning stage preceded, the indirect tension modulus software charted and tabulated the displacement and force. The out-of-range LVDTs were adjusted, and to conclude the test automatically, five pulses of nearly constant deformation were applied by closing the level display.

The dynamic modulus test was conducted according to AASHTO TP 62-07. The in- process control (IPC) Global Simple Performance Tester (GSPT), also known as the Asphalt Mix Performance Tester (AMPT), was used to determine dynamic modulus (Zhu et al., 2020). The specimens were prepared to the required dimensions, and gauge points were fixed using epoxy glue, as shown in Figure 3a. These gauge points were fixed to attach LVDTs to measure the axial deformation/strain for the specimens during the test. The clamps were fixed to the specimens after removing them from the water bath. These clamps were designed to accommodate LVDTs for measuring the deformations (Figure 3b).

The specimens were placed in the environmental chamber and allowed to equilibrate to the target test temperature within ± 0.5°C. Each specimen was tested at 25°C using frequencies of 25, 10, 5, 0.5, and 0.1 Hz, respectively. A continuous uniaxial sinusoidal compressive stress was applied to the unconfined cylindrical test specimen. The deformation of the specimen was captured using linear variable displacement transducers mounted 120° apart. The software automatically generated the results at the test's completion, and the dynamic modulus values were reported against the given temperature and corresponding test frequencies.

3 Results and Discussion

3.1 Volumetric Properties of Mix Having 3%, 6%, and 9% Fines

To determine the optimum asphalt contents of mix having 3%, 6%, and 9% fines, the graphs between asphalt contents and volumetric properties, stability, and flow were plotted according to the MS-2 manual (Radeef et al., 2022). The asphalt contents at 4% air void are considered optimum asphalt contents. The mix containing 3% fines has an optimum asphalt content of 4.1%. The values of volumetric properties, stability, and flow according to the optimum asphalt contents were observed from the graphs. Table 3 shows the job mix formula of the mixture, which has 3% fines. It also shows that the volumetric properties, stability, and flow meet the criteria. VMA at 4% design air void should not be less than 14%; in this case, its value was 14.1%. VFA was found to be 71, which should be between 65 and 75. Similarly, the stability value was 8630, which should not be less than 8006 N based on the given criterion, and the measured value of the flow number was 2.55 (Table 3).

Table 3: Job mix formula observations for mix having 3%, 6%, and 9% fines (ASTM Standard, D-3515,2014).

Parameters	Criteria	Measured Value			Remarks (3%/6%/9%)
		3% fines	6% fines	9% fines	
Optimum asphalt content (%)	NA	4.10	4.45	5.00	P/P/P
VMA (%)	14	14.10	14.10	16.60	P/P/P
VFA (%)	65–75	71.00	71.00	71.00	P/P/P
Stability (N)	8006	8630	8465	8110	P/P/P
Flow (mm)	2.0–3.5	2.55	2.85	3.10	P/P/P

P stands for pass; F stands for fail

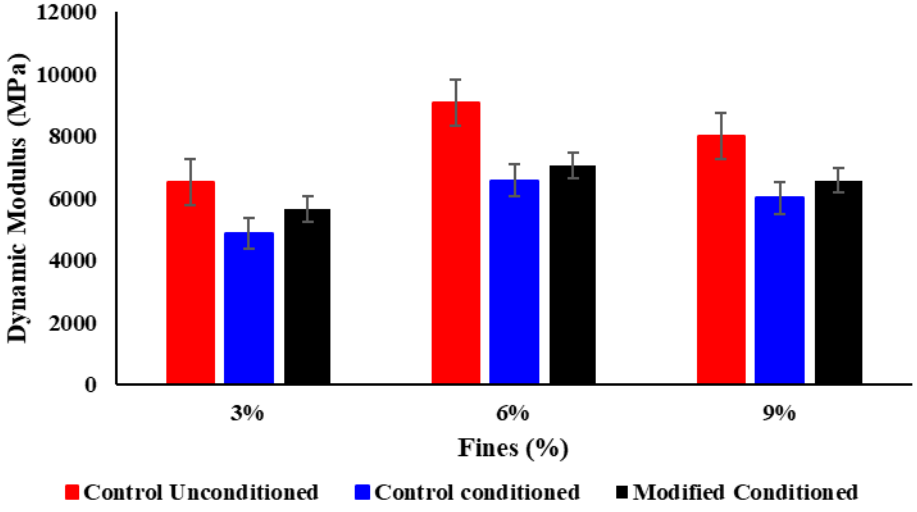

Figure 4: Measured dynamic modulus of asphalt concrete mixtures with 3%, 6%, and 9% fines with and without freeze–thaw conditioning.

The mix containing 6% fines had an optimum asphalt content of 4.45%. Table 3 also shows the job mix formula of a mixture having 6% fines. VMA and VFA were observed to be 14.10% and 71, respectively. The stability value was 8465 N, and the measured value of the flow number was 2.85, which met the criteria limit (Table 3). The mix design having 9% fines had an optimum asphalt content of 5%, illustrating that VMA and VFA were 16.60% and 71, respectively, at 4% design air voids. On the other hand, the stability value and the flow number were observed to be 8110 and 3.10, respectively, which meet the criteria (Table 3).

3.2 Dynamic Modulus Test

The dynamic modulus test data, analyzed using 18 data values, provides insights into the moisture susceptibility of the mixtures. Figure 4 illustrates the dynamic modulus of the mixture at a test frequency of 10 Hz. It is evident that for all specimens, a drop in modulus was observed after conditioning. Notably, mixtures with 6% fines, whether conditioned or not, generally exhibited higher dynamic modulus. This can be attributed to the role of hydrated lime in modifying the dynamic modulus. For all three cases, 3%, 6%, and 9% fine lime modification improved the dynamic modulus by 20%, 10%, and 14%, respectively.

3.2.1 Indirect Tensile Strength Test

A total of nine specimens were prepared for the indirect tensile test. These specimens were sliced thrice: one for the indirect tension test and two for the resilient modulus test. Figure 5 presents the indirect tensile strength, showing that the mixtures with 6% fines produced the highest indirect tensile strength before and after conditioning compared to mixtures with 3% and 9% fines. The reduction in strength

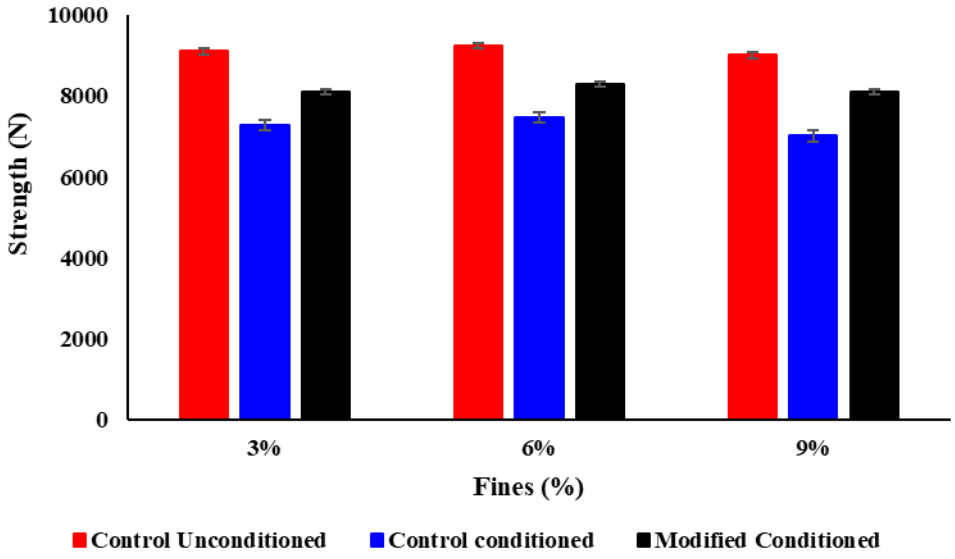

Figure 5: IDT strength of asphalt concrete mixtures with 3%, 6%, and 9% fines with and without freeze–thaw conditioning.

due to conditioning is less for antistripped specimens than for control-conditioned specimens (Zhang & Luo, 2019). The effect of hydrated lime is more on the mixture with 6% fines. This also indicates a slight difference in strength of mixtures with 3% and 9% fines for control-unconditioned and control-conditioned specimens. The improvements of indirect strength due to lime modification for 3%, 6%, and 9% fines are 11%, 12%, and 10%, respectively (Figure 5).

3.3 Resilient Modulus Test

Figure 6 shows that the resilient modulus is higher for the mixture having 6% fines compared to the other two types of mixtures. The effect of conditioning and hydrated lime is also more significant on the resilient modulus than the dynamic modulus and indirect tensile strength. The improvement of resilient modulus due to lime modification for mixtures with 3%, 6%, and 9% fines is 54%, 32%, and 68%, respectively. It is observed that the improvement in resilient modulus, dynamic modulus, and tensile strength values decreases initially at 6% fines and then increases again at 9% fines. The probable cause of this trend in 3% fines mixture could be attributed to the available amount of hydrated lime and fines converted into Pozzolanic compound due to the reaction between pozzolana and calcium ion (Ca^{+2}) in the presence of water, which enhances the resilient modulus, dynamic modulus, and tensile strength (Barman & Dash, 2022). At 9% fines, the modified mix's behavior is controlled by the mastic (fines + binder), and all available fines are not converted into Pozzolanic compound. Moreover, 6% fines aggregates have better particle-to-particle contacts, resulting in higher resilient modulus, dynamic modulus, and tensile strength.

3.4 Effectiveness of Different Parameters for Moisture Susceptibility

The effectiveness and comparison of different parameters for evaluating laboratory-measured moisture susceptibility are presented in Table 4. The ratios of parameters of asphalt concrete mixtures conditioned to unconditioned and modified conditioned to unconditioned were calculated for different proportions of fines with 3%, 6%, and 9%. The strength and resilient modulus of the mixture having 6% fines with and without lime modification are higher than those of mixtures with 3% and 9% fines. According to the Superpave mix design, the ratio of parameters for moisture susceptibility should be greater than or equal to 80. Table 4 shows that all the tested mixes are prone to moisture damage/stripping and require some modification. Only 6% fines mixture's indirect strength test without lime modification meets the criteria. The improvements of 3%, 6%, and 9% fines mixture's moisture susceptibility due to lime modification considering the dynamic modulus are 11%, 7%, and 11%, respectively. The improvements of 3%, 6%, and 9% fines mixture's moisture susceptibility due to lime modification considering indirect tensile strength are 9%, 9%, and 8%, respectively. The lime modification effect is higher

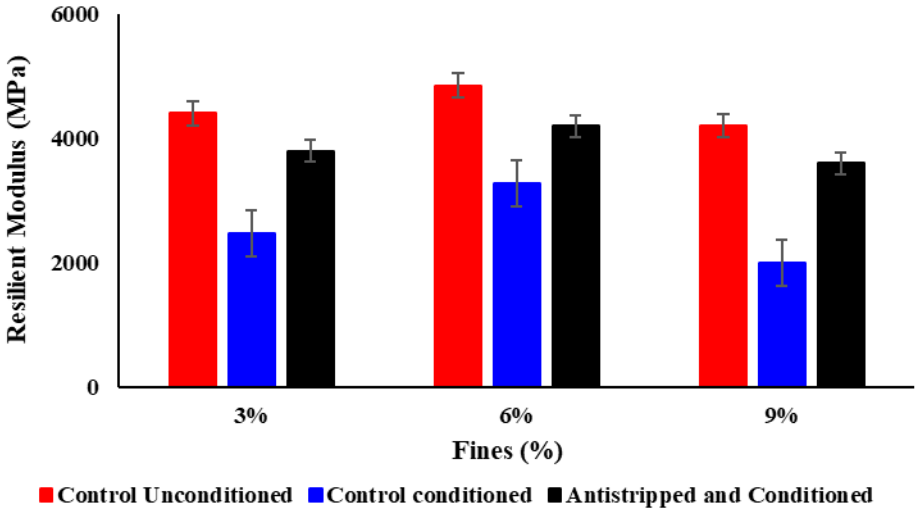

Figure 6: Measured resilient modulus of asphalt concrete mixtures with 3%, 6%, and 9% fines with and without freeze–thaw conditioning.

Table 4: Comparison of different parameters for moisture susceptibility.

Fines (%)	Conditioning	Dynamic modulus ratio at 10 (Hz)		Tensile strength ratio		Resilient modulus ratio	
		Without AS	With AS	Without AS	With AS	Without AS	With AS
3%	One cycle F-T	74	85	78	87	56	87
6%	One cycle F-T	74	81	80	89	68	90
9%	One cycle F-T	69	80	77	85	51	86

Table 5: Factor's notations and their levels for analysis.

Factors	Notation	Levels	
Frequency (Hz)	A	0.1	25
Fines (%)	B	3	9
Conditioning	C	Conditioned	Unconditioned

for resilient modulus compared to dynamic modulus and indirect tensile strength. The improvements of 3%, 6%, and 9% of the fine mixture's moisture susceptibility due to lime modification considering resilient modulus are 31%, 22%, and 35%, respectively.

3.5 Full Factorial Design for Dynamic Modulus

The analysis of dynamic modulus data for the control-unconditioned and -conditioned specimens was carried out by considering three factors, that is, frequency, percentage of fines, and freeze–thaw conditioning, each with two levels. Therefore, 23 full factorial designs of the experiment were adopted using Minitab-15 software. Table 5 shows the factors considered in the 23 full factorial designs of the experiment, with their notations illustrating low and high severity levels. Inputting these three factors into software resulted in eight combinations. Each experimental condition was replicated twice to obtain a reasonable estimate of error. Furthermore, Table 6 predicts the combination of factors generated by the software for the complete factorial design of the experiment.

3.5.1 Effects and Coefficient Table

The factors and interaction of factors with high values of effect and coefficient indicate that they significantly impact the dynamic modulus of HMA. The effect of each term is equal to the twice of the coefficient. The calculated value of t-statistics of all the terms is greater than the critical value of t-statistics (t-critical = 2.001 for the degree of freedom 63 and significance level of 5%), and the p-value of all individual factors and interaction of factors is less than the significance level, which shows that all the factors and their interactions are significant at 5% significance level.

Table 6: Measured values of dynamic modulus with different percent fines and frequency.

Frequency (Hz)	Fines (%)	Conditioning	Dynamic modulus (MPa)
0.1	3	Conditioned	805
0.1	3	Conditioned	1036
0.1	9	Conditioned	1100
25	3	Conditioned	5704
25	3	Unconditioned	7474
25	3	Conditioned	6268
25	9	Conditioned	7501
0.1	9	Conditioned	845
25	9	Unconditioned	10.376
25	9	Conditioned	7091
0.1	3	Unconditioned	963
0.1	9	Unconditioned	1423
25	9	Unconditioned	10.508
25	3	Unconditioned	7124
0.1	3	Unconditioned	966
0.1	9	Unconditioned	1550

3.5.2 Significant Effects and Interaction Plots

The most significant effects and the dynamic modulus of bituminous paving mix are illustrated with the Pareto plot, half-normal probability plot, and normal probability plot obtained using Minitab-15 software (Figures 7, 8, and 9, respectively). Figure 7 shows the Pareto plot with the absolute effects values, and a reference line drawn indicates the critical value of student- t. It is interesting to note that all the main factors, such as the frequency, fines and conditioning, and interactions, i.e., the 2-way interactions of frequency and fines, fines and conditioning, frequency and conditioning and the 3-way interaction of frequency, are beyond the reference line, which shows that all the main factors and their interactions are significant at 5% significance level. The Pareto plot shows that the frequency is the most significant factor when its level changes from 0.1 to 25. The fines and conditioning have a similar effect at a 5% significance level.

Figures 8 and 9 illustrate the half-normal probability plot and normal probability plot of standardized effects, respectively. The significant effect from the half-normal probability plot or normal probability plot is evidence of how far a factor or interaction of factors is from the

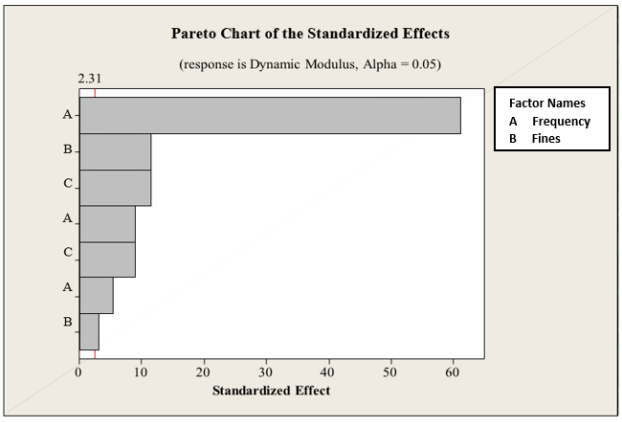

Figure 7: Pareto plot illustrating standardized effects.

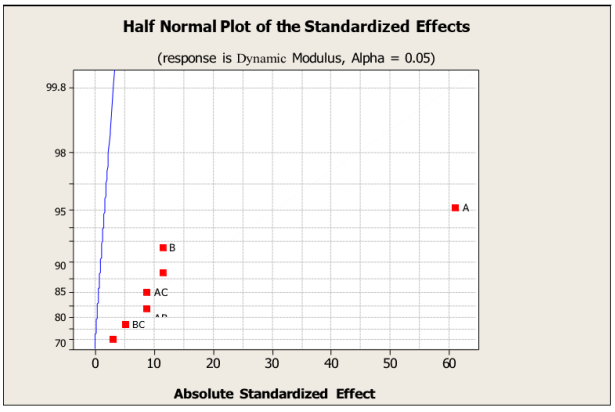

Figure 8: Visualization of absolute standardized effects in the half-normal plot.

reference line. Both plots show that at a 5% significance level, all the factors and their interactions are significant, but frequency is the most significant factor affecting the dynamic modulus test.

3.5.2.1 Main Effect Plots

Figure 10 shows the effects of frequency, fines, and conditioning and illustrates that the dynamic modulus is much higher at 25 Hz compared to 0.1 Hz. With increased frequency, more stresses are absorbed in the specimen, ultimately raising the dynamic modulus. The fines plot shows the effect of fines on the dynamic modulus of bituminous paving mixes. The larger dynamic modulus occurs for specimens with 9% fines, while the dynamic modulus is lower for specimens with 3% fines. The mix of 3% fines has more void spaces in the aggregate matrix compared to the mix of 9% fines, which lowers the dynamic modulus. The conditioning plot shows a slope

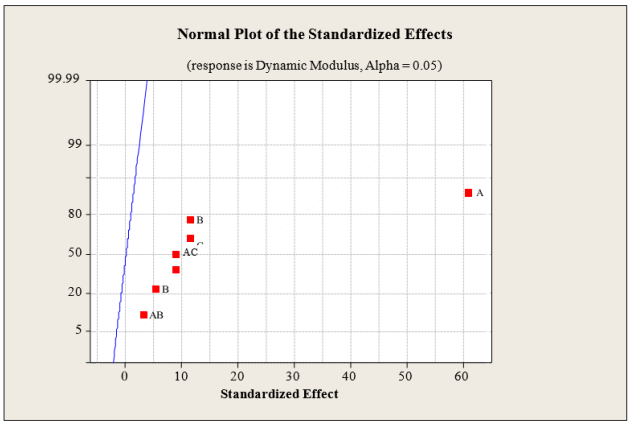

Figure 9: Visualization of the standardized effect of the normal plot.

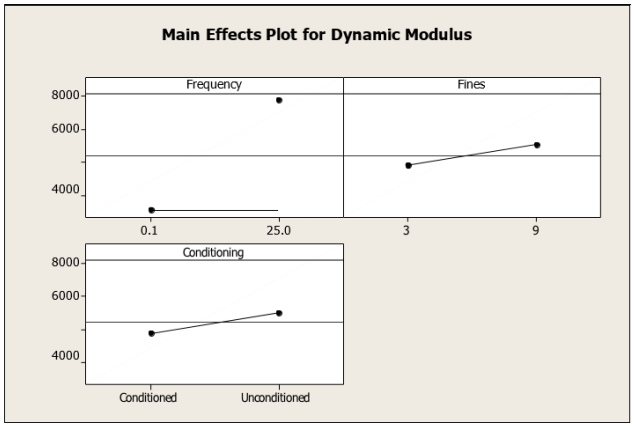

Figure 10: Main effects plot for dynamic modulus.

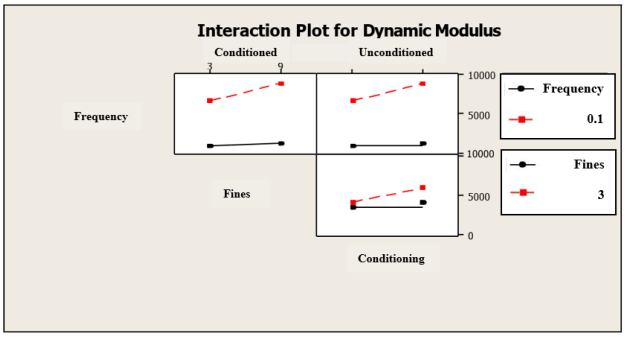

Figure 11. Interaction plots for dynamic modulus.

similar to the fines plot. The dynamic modulus is lower for the control-conditioned specimens and higher for the control-unconditioned specimens. Because of the freeze–thaw cycle, the specimens become saturated due to the absorption of water, which automatically lowers their stiffness potential.

3.5.2.2 Interaction Plots

Figure 11 shows that all the interactions – frequency and fines, fines and conditioning, and frequency and conditioning – are significant and represented by nonparallel lines. The most significant two-way interaction is fines and conditioning. It is observed that the effect of fines is most prominent in unconditioning. The combination of higher fines and unconditioning. results in a higher value of dynamic modulus. At conditioning, 3% and 9% fine specimens show almost the same dynamic modulus. Figure 11 also shows that for 3% fines specimens, when the frequency is 0.1 Hz, there is a very small variation in dynamic modulus values. Similarly, conditioned and unconditioned samples for 0.1 Hz frequency have shown similar dynamic modulus. At 25 Hz frequency, the dynamic modulus is higher at 9% fines and unconditioning compared to 3% fines and conditioning.

3.5.2.3 Cubic Plot

The cubic plot for the dynamic modulus illustrates that the maximum dynamic modulus value is observed at 25 Hz frequency for 9% fines when the specimen is unconditioned (Figure 12). This could be attributed to small deformation occurring during this condition, which produces a deficient strain and, hence, results in the highest dynamic modulus. The value of dynamic modulus is lowest for the conditioned specimens at 3% fines and 0.1 Hz frequency. Due to fewer fines, the mix contains many void spaces, resulting in higher strain production and ultimately reducing the dynamic modulus for this condition.

3.6 Analysis of Variance

In an analysis of variance (ANOVA), three F-tests are prepared, and the probability values for evaluating these tests are presented in Table 7. The initial three tests observed the significance of individual factors, 2-way interactions, and 3-way interactions. p-value <0.05 shows that these tests are satisfied.

3.7 Regression Analysis for Resilient Modulus

Regression analysis of dynamic modulus data has also been performed for control-unconditioned, control-conditioned, and antistripped with conditioned specimens by considering dynamic modulus as the response variable

Table 7: Analysis of variance for dynamic modulus.

Sources	DF	SS	MSS	F-test	*p*-value
Main effects	3	190,552,515	63,517,505	1336.0	0.000
2-way interactions	3	8,892,063	2,964,021	62.35	0.000
3-way interactions	1	464,442	464,442	9.77	0.014
Residual error	8	380,322	47,540		
Total	1	200,289,341	47,540		

MSS: mean sum of square, SS: sum of square

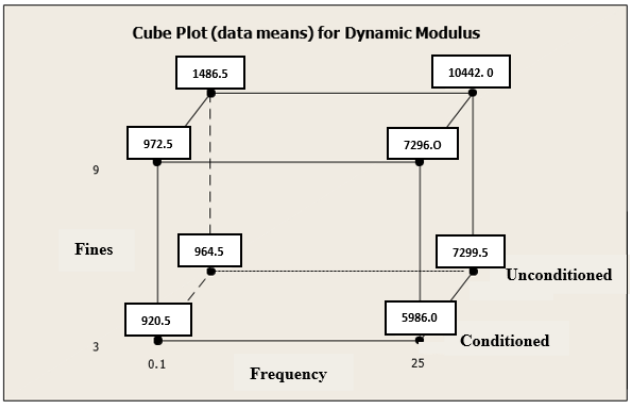

Figure 12: Cube plot for dynamic modulus.

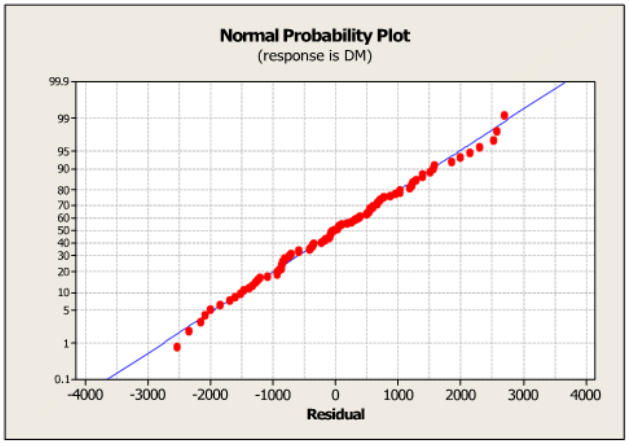

Figure 13: Typical normal probability plot.

and frequency as well as fines as predictors. The number of data values used in the regression analysis was 89. The regression equation (Equation 1) is as follows:

$$\text{dynamic modulus} = 1363 + 173^{*}\ \%\ \text{fines} + 277\ ^{*}\text{loading frequency} \quad (1)$$

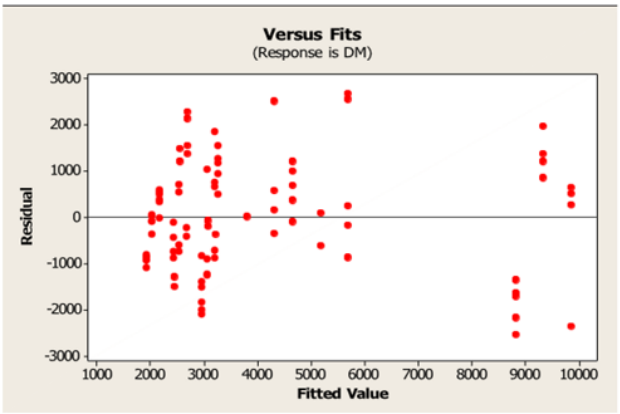

Figure 14: Typical residual versus fitted values.

The value of R^2 for this model is 80%, which is a good fit. Figure 13 shows the normal probability plot of residuals; the normality assumption is satisfied because the plot demonstrates a straight line, which shows that the errors are normally distributed. Figure 14 also indicates that the residuals are structure less and the plotted points made an approximately horizontal band that satisfies the assumption. However, the correlation between the residuals is detected by plotting the residuals in the time order of data collection. Figure 15 indicates that the residuals are independent and unrelated, while the indefinite pattern of the plot shows that it is structureless.

3.8 Model Validation

The model was validated using the mean absolute percentage error (MAPE), which is defined as the percentage deviation of the predicted value from the observed value for a fitted time series (Alim et al., 2020). MAPE is generally expressed in percentages and can be formulated using Equation 2.

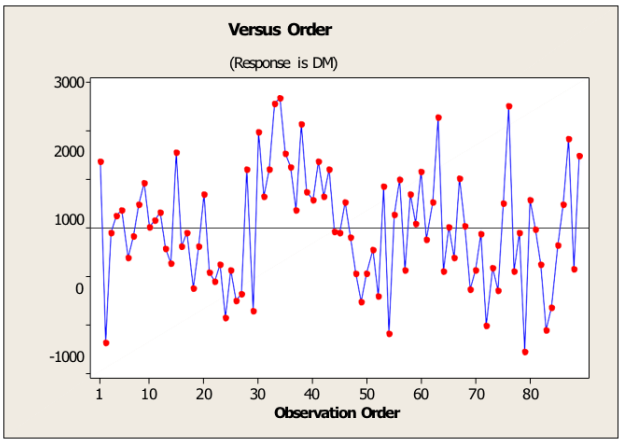

Figure 15: Typical residual versus fitted values.

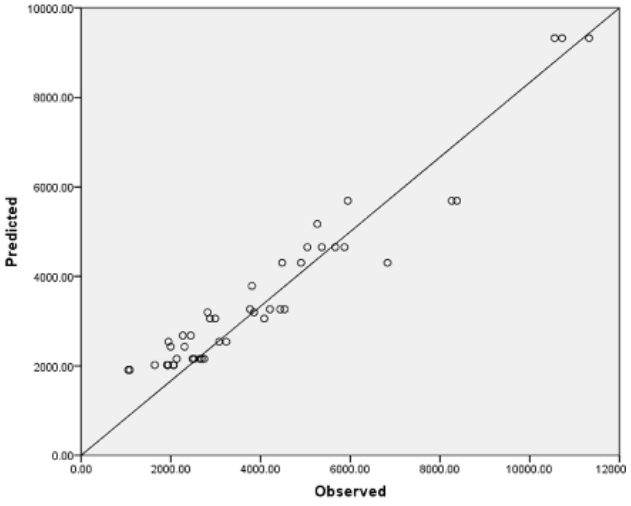

Figure 16: Validation plot between predicted and observed values.

$$SD = \frac{1}{N}\left(\begin{matrix} n \\ > \\ i \end{matrix}\right)\left(\frac{\text{Observation} - \text{Predicted}}{\text{Observation}}\right) \quad (2)$$

where SD is the standard deviation and N is the number of values.

Before the development of the model, 50% of the data was randomly selected for validation of the developed model. The model's predictive capability can be tested by calculating MAPE using model parameters and validation data set (Pradhan, 2013). The MAPE value was 9 for the validation data set, which is satisfactory; hence, the model is a significant fit. The observed versus predicted values were plotted as shown in Figure 16, demonstrating the model's predictive capability. The model for which predicted data points were close to the 100% validation line was considered the best predictive.

4 Conclusions

A comprehensive investigation was conducted to determine the effectiveness of different proportions of fines and hydrated lime in asphalt concrete mixtures used in Pakistan, focusing on their impact on moisture susceptibility. Moisture susceptibility poses a significant challenge for ACPs, and lime modification emerged as a highly effective strategy for mitigating this concern.

The optimal asphalt content was established for mixtures with 3%, 6%, and 9% fines, revealing that the mixtures met the volumetric properties, stability, and flow criteria. The optimum contents were 4.1%, 4.45%, and 5% for 3%, 6%, and 9% fines, respectively. However, the dynamic modulus of the mixtures improved with the incorporation of hydrated lime, particularly for the 6% fines mixture. This mixture exhibited the highest dynamic modulus before and after conditioning, with lime modifications enhancing the modulus by 20%, 10%, and 14% for 3%, 6%, and 9% fines, respectively. In addition, 6% fines demonstrated the highest indirect tensile strength, showing a notable resistance to strength reduction after conditioning. In comparison, the resilient modulus was significantly higher in mixtures with 6% fines, with lime modification showing the most substantial impact. Evaluations of moisture susceptibility revealed that lime modification substantially mitigated moisture damage across all mixtures.

Adding 1.5% hydrated lime based on the dry weight of aggregates proved instrumental in enhancing the strength and stiffness of the asphalt concrete mixtures and reducing moisture susceptibility. However, it is essential to note that the three types of mixtures examined in this research fell short of meeting the Superpave mix design criteria for moisture susceptibility evaluation, indicating vulnerability to stripping with a tensile strength ratio (TSR) below 80%. For all three cases of mixtures under consideration, lime modification led to substantial improvements in dynamic modulus (20%, 10%, and 14%, respectively), indirect tensile strength (11%, 12%, and 10%, respectively), and resilient modulus (54%, 32%, and 68%, respectively).

Furthermore, a thorough analysis using 23 full factorial designs of the experiment revealed that individual factors were significant, and the interactions among these factors also played a crucial role. Loading frequency emerged as the most significant factor for dynamic modulus, with a notable influence when its level varied from 0.1 to 25 Hz. In addition, the interaction between fines and conditioning proved particularly noteworthy, emphasizing the nuanced

effects of fines on control-unconditioned specimens versus conditioned specimens.

In summary, the practical aspects of the research, which are directly applicable in real-world scenarios, encompass optimizing mix designs, mitigating moisture susceptibility, implementing findings in pavement construction, considering cost-effectiveness, and monitoring long-term performance. These aspects are not just crucial, but also highly relevant for improving the durability and resilience of ACPs.

Availability of Materials

All the required data is provided in the manuscript.

Conflicts of Interest

The authors declare no conflict of interest.

Ethical Rules

Not applicable.

References

[1] Abed, A. H., Qasim, Z. I., Al-Mosawe, H., & Norri, H. H. (2019). The effect of hybrid anti-stripping agent with polymer on the moisture resistance of hot-mix asphalt mixtures. *Cogent Engineering*, *6*(1), 1659125. https://doi.org/10.1080/23311916.2019.1659125

[2] Al-Tameemi, A. F., Wang, Y., & Albayati, A. (2015). Influence of hydrated lime on the properties and permanent deformation of the asphalt concrete layers in pavement. *Romanian Journal of Transport Infrastructure*, *4*(1), 1–19. https://doi.org/10.1515/rjti-2015-0027

[3] Alam, M. N., & Aggarwal, P. (2020). Effectiveness of anti stripping agents on moisture susceptibility of bituminous mix. *Construction and Building Materials*, *264*, 120274. https://doi.org/10.1016/j.conbuildmat.2020.120274

[4] Alim, M., Ye, G.-H., Guan, P., Huang, D.-S., Zhou, B.-S., & Wu, W. (2020). Comparison of ARIMA model and XGBoost model for prediction of human brucellosis in mainland China: a time-series study. *BMJ Open*, *10*(12). https://doi.org/10.1136/bmjopen-2020-039676

[5] Asmara, Y. (2024). (2023). Introduction to Reinforced Concrete. In *Concrete Reinforcement Degradation and Rehabilitation. Engineering Materials*. Springer, Singapore. https://doi.org/10.1007/978-981-99-5933-4_1

[6] ASTM. (2020). *Standard Practice for Preparation of Asphalt Mixture Specimens Using Marshall Apparatus*. https://www.astm.org/d6926-20.html

[7] ASTM, A. (2011). Standard test method for theoretical maximum specific gravity and density of bituminous paving mixtures. *American Society for Testing an d Materials, West Conshohocken, PA*.

[8] ASTM International. (2021). *Standard Test Method for Bulk Specific Gravity and Density of Non-Absorptive Compacted Asphalt Mixtures*. https://www.astm.org/d2726_d2726m-21.html

[9] Barman, D., & Dash, S. K. (2022). Stabilization of expansive soils using chemical additives: A review. *Journal of Rock Mechanics and Geotechnical Engineering*, *14*(4), 1319–1342. https://doi.org/10.1016/j.jrmge.2022.02.011

[10] Bashir, M. T., Muhammad, S., Butt, M. J., Alzara, M., & El-kady, M. S. (2020). Aspect ratio effect of multi-walled carbon nanotubes and carbon fibers on high-performance cement mortar matrices. *Innovative Infrastructure Solutions*. https://doi.org/10.1007/s41062-020-00290-2

[11] Brown, E. R., & Foo, K. Y. (1989). *Evaluatıon of Varıabılllty in Resilient Modulus Test Results (ASTM D 4123-82*. NCAT Report.

[12] Cong, P., Guo, X., & Ge, W. (2021). Effects of moisture on the bonding performance of asphalt-aggregate system. *Construction and Building Materials*, *295*, 123667. https://doi.org/https://doi.org/10.1016/j.conbuildmat.2021.123667

[13] Diab, A., & Enieb, M. (2018). Investigating influence of mineral filler at asphalt mixture and mastic scales. *International Journal of Pavement Research and Technology*, *11*(3), 213–224. https://doi.org/https://doi.org/10.1016/j.ijprt.2017.10.008

[14] Faramarzi, M., Golestani, B., & Lee, K. W. (2017). Improving moisture sensitivity and mechanical properties of sulfur extended asphalt mixture by nano-antistripping agent. *Construction and Building Materials*, *133*, 534–542. https://doi.org/https://doi.org/10.1016/j.conbuildmat.2016.12.038

[15] Ghani, U., Zamin, B., Tariq Bashir, M., Ahmad, M., Sabri, M. M. S., & Keawsawasvong, S. (2022). Comprehensive study on the performance of waste HDPE and LDPE modified asphalt binders for construction of asphalt pavements application. *Polymers*, *14*(17), 3673. https://doi.org/10.3390/polym14173673

[16] Guo, F., Pei, J., Zhang, J., Li, R., Liu, P., & Wang, D. (2022). Study on adhesion property and moisture effect between SBS modified asphalt binder and aggregate using molecular dynamics simulation. *Materials*, *15*(19), 6912. https://doi.org/10.3390/ma15196912

[17] Kalaitzaki, E., Kollaros, G., & Athanasopoulou, A. (2017). Significance of Fines in Hot Mix Asphalt Synthesis. *Romanian Journal of Transport Infrastructure*, *6*(1), 30–42. https://doi.org/10.1515/rjti-2017-0052

[18] Karimi, H. R., Khedri, E., Aliha, M. R. M., Shaker, H., & Haghighatpour, P. J. (2023). Repair efficiency evaluation for cracked asphalt mixture pavement in different ambient temperatures using bitumen and polymer concrete as repair materials. *Construction and Building Materials*, *369*, 130556. https://doi.org/https://doi.org/10.1016/j.conbuildmat.2023.130556

[19] Kaseer, F., Martin, A. E., & Arámbula-Mercado, E. (2019). Use of recycling agents in asphalt mixtures with high recycled materials contents in the United States: A literature review.

Construction and Building Materials, *211*, 974–987. https://doi.org/https://doi.org/10.1016/j.conbuildmat.2019.03.286

[20] Park, D.-W., Seo, W.-J., Kim, J., & Vo, H. V. (2017). Evaluation of moisture susceptibility of asphalt mixture using liquid anti-stripping agents. *Construction and Building Materials*, *144*, 399–405. https://doi.org/10.1016/j.conbuildmat.2017.03.214

[21] Pezowicz, P., & Choma-Moryl, K. (2015). Moisture content impact on mechanical properties of selected cohesive soils from the wielkopolskie voivodeship southern part. *Studia Geotechnica et Mechanica*, *37*(4), 37–46. https://doi.org/10.1515/sgem-2015-0043

[22] Pradhan, B. (2013). A comparative study on the predictive ability of the decision tree, support vector machine and neuro-fuzzy models in landslide susceptibility mapping using GIS. *Computers & Geosciences*, *51*, 350–365. https://doi.org/10.1016/j.cageo.2012.08.023

[23] Radeef, H. R., Hassan, N. A., Katman, H. Y., Mahmud, M. Z. H., Abidin, A. R. Z., & Ismail, C. R. (2022). The mechanical response of dry-process polymer wastes modified asphalt under ageing and moisture damage. *Case Studies in Construction Materials*, *16*, e00913. https://doi.org/10.1016/j.cscm.2022.e00913

[24] Standard, A. (2015). Standard test method for marshall stability and flow of asphalt mixtures. *West Conshohocken, PA*.

[25] Sukhija, M., Saboo, N., & Pani, A. (2023). Effect of warm mix asphalt (WMA) technologies on the moisture resistance of asphalt mixtures. *Construction and Building Materials*, *369*, 130589. https://doi.org/https://doi.org/10.1016/j.conbuildmat.2023.130589

[26] Tang, Y., Fu, Z., Ma, F., Zhao, P., Hou, Y., Jiang, X., & Peng, C. (2023). Effect of water molecular behavior on adhesion properties of asphalt-aggregate interface. *Construction and Building Materials*, *402*, 133028. https://doi.org/https://doi.org/10.1016/j.conbuildmat.2023.133028

[27] Ye, Y., Hao, Y., Zhuang, C., Shu, S., & Lv, F. (2022). Evaluation on improvement effect of different anti-stripping agents on pavement performance of granite–asphalt mixture. *Materials*, *15*(3), 915. https://doi.org/10.3390/ma15030915

[28] Zhang, D., & Luo, R. (2019). Using the surface free energy (SFE) method to investigate the effects of additives on moisture susceptibility of asphalt mixtures. *International Journal of Adhesion and Adhesives*, *95*, 102437. https://doi.org/10.1016/j.ijadhadh.2019.102437

[29] Zhu, J., Ghafoori, E., & Dinegdae, Y. (2020). *Characterization of asphalt mixtures and bitumen to minimize shear-related distresses in asphalt pavement*.